

USING CTX-BASED CRATER SIZE-FREQUENCY DISTRIBUTIONS TO REFINE THE GEOLOGIC HISTORY OF DEUTERONILUS MENSAE, MARS. Emily C.S. Joseph, David A. Crown, Daniel C. Berman, Frank C. Chuang, Planetary Science Institute, 1700 E. Ft. Lowell Rd., Suite 106, Tucson, AZ 85719; crown@psi.edu.

Introduction: With the availability of new high-resolution images for Mars, crater size-frequency distributions can be extended to smaller craters, providing new insights into the erosional and depositional histories of geologic units as well as refinements of formation ages. Along the dichotomy boundary in Deuteronilus Mensae, model ages derived for various geologic units are being used to provide important temporal constraints on the formation of the highland-lowland boundary, development of fretted terrain, and emplacement of lobate debris aprons. Deuteronilus Mensae exhibits a variety of geologically young, ice-related features, including ice-cemented mantling deposits, lobate debris aprons, concentric crater fill, and lineated valley fill that are key indicators of past climate conditions. Preliminary results using Mars Reconnaissance Orbiter Context Camera (CTX; ~5 m/pixel) images on the ejecta blankets of several craters in Deuteronilus Mensae (including Cerulli crater), debris aprons, plains, and plateau units are presented here.

Geology of Deuteronilus Mensae: Our analyses focused on three mapped Mars Transverse Mercator (MTM) quadrangles (35337, 40337, and 45337; 32.5-47.5°N, 20-25°E) that transect the dichotomy boundary in Deuteronilus Mensae [1-3]. The map [3] identified 11 geologic units, which can be grouped into four material types (from oldest to youngest): plateau, plains, impact crater, and surficial materials.

From photogeologic interpretation of the area and age constraints using initial crater counts on Viking, THEMIS IR and HRSC images [3] (Figure 1), the map area was dominated by the highland plateau during the Noachian Period; the plateau likely extended from its current locations in the south across the entire transect. The plateau was then broken down by subsequent tectonic, fluvial, and impact activity. Deeper layers of the plateau were exposed by erosion in the Late Noachian or Early Hesperian Epochs and degradation of plateau materials eventually led to the formation of polygonal mesas, knobs, and fretted valleys that are observed north of the continuous plateau margin. By the end of the Hesperian Period, the plateau had further degraded, with extensive plains forming in low-lying regions.

In the Amazonian Period, ice-driven resurfacing occurred, resulting in a variety of landforms that modified and subdued the landscape, including lobate debris aprons, concentric crater fill, and smooth fill

deposits. Lobate debris aprons appear to have formed in cycles in the Early/Middle Amazonian. The most recent activity was the deposition and partial removal of ice-rich mantling deposits.

Crater Count Methodology: To test and refine age interpretations based on geologic mapping and previous crater counts, crater size-frequency distribution statistics have been compiled from CTX images using established methodologies [4-7]; all impact craters (primaries and isolated secondaries) on a given surface in a specific diameter range were counted while avoiding areas of obvious secondary chains or clusters. These data were then plotted on the isochrons defined by [5-7] to assess both relative (Martian time-stratigraphic age) and absolute ages. Deviations from isochron shape over specific crater size ranges may provide information on erosional and depositional processes affecting the surfaces of interest.

Crater size-frequency distributions from CTX images have been analyzed for upper and lower plateau units, debris aprons, and plains units, as well as for debris aprons and superposed ejecta of a 22-km-diameter crater at 42.1°N, 23.4°E, and the highland plateau and nearby ejecta blanket of Cerulli crater (32.2°N, 22.0°E) (Figure 2).

Results: The distributions of all craters superposed on the upper and lower plateaus and the smooth plains unit match the slope of the isochrons at diameters between ~500 m and 3 km with a departure at sizes smaller than ~500 m (Figure 3). In this diameter range, the Noachian plateau units show the effects of Hesperian surface modification, with the upper plateau units showing modification in the Late Noachian/Early Hesperian, and the lower plateau units showing modification during the Early to Late Hesperian. The Hesperian/Noachian smooth plains unit shows surface modification ages in this diameter range during the Late Hesperian/Early Amazonian. The distribution of all craters superposed on the debris aprons match the isochrons at diameters between 750 m and 4 km, with a departure at sizes smaller than 750 m. Formation age for the debris aprons is interpreted to be ~1 Gy, during the Early Amazonian.

The preferential loss of small craters within these units is consistent with cycles of deposition of ice-rich mantling deposits during periods of high obliquity. The diameter at which this depletion begins (~250 – 750 m depending on unit) gives an indication of the depth to which this mantle has been preserved (for further

discussion of this effect on the craters see companion abstract by Berman et al. [8]).

Conclusions: Compilation of crater size-frequency distributions from analysis of CTX images provides important temporal information regarding Martian geologic units, extending characterization down to < 100 m. These analyses provide information on both formation ages and the timing and nature of degradational processes in the Deuteronilus Mensae region. Our results are consistent with those from geologic mapping and have resulted in refinement of unit ages.

References: [1] Chuang F.C. and Crown D.A. (2006) *LPSC 37*, Abstract #1332. [2] Chuang F.C. and Crown D.A. (2006) *EOS Trans. AGU 87(52)*, abstract P31B-01. [3] Chuang, F.C., and D.A. Crown (2009) USGS Sci. Invest. Ser. Map 3079. [4] Berman D.C. and Hartmann W.K. (2002) *Icarus*, 159, 1-17. [5] Hartmann W.K. (2005) *Icarus*, 174, 294-320. [6] Hartmann W.K. (2007) *7th Intl. Conf. on Mars*, Abstract #3318. [7] Hartmann, W.K. (2007) *Icarus*, 189, 274-278. [8] Berman D.C. et al. (2011) *Lunar Planetary Sci. Conf. 42*, this conference.

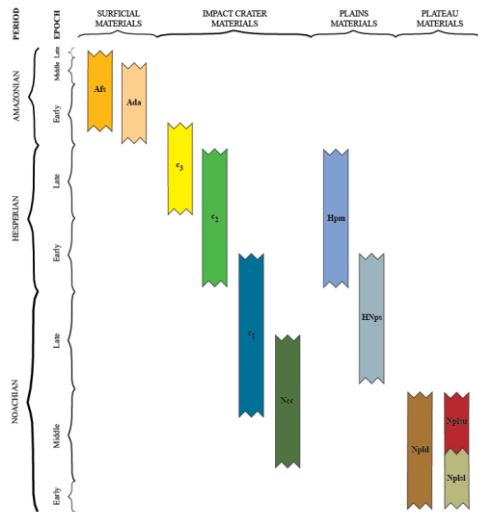


Figure 1. Diagram showing stratigraphic correlation of map units from [3]. Vertical extents of unit bars determined by photogeologic analyses and crater statistics using Viking, THEMIS IR and HRSC images.

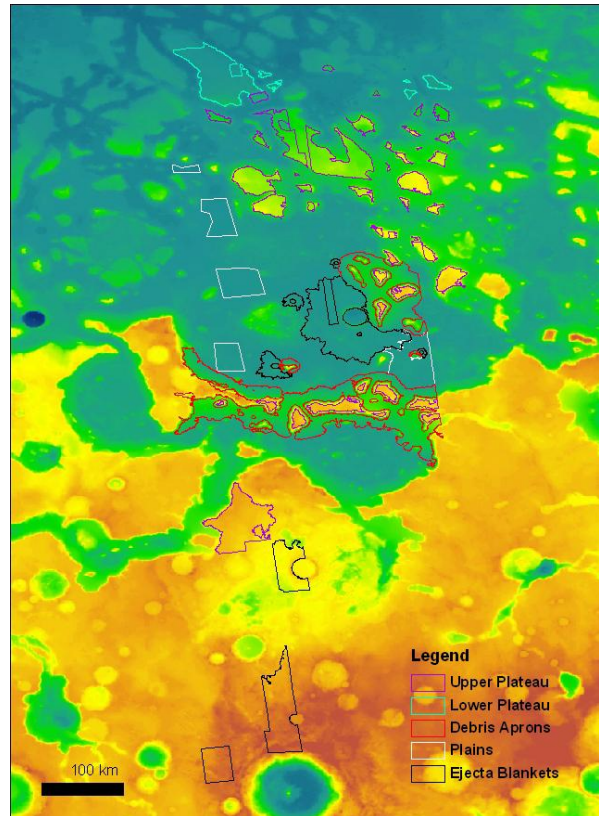


Figure 2. MOLA 128 pixel/degree map showing crater count areas on various geologic units.

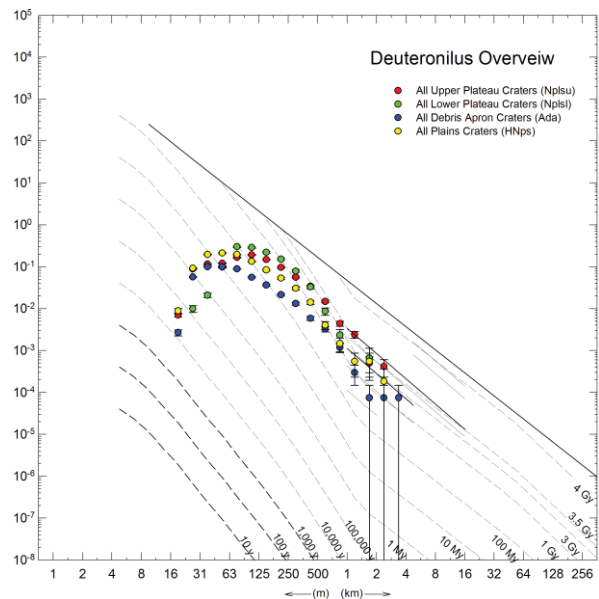


Figure 3. Crater size-frequency distributions from CTX images of Deuteronilus Mensae. Upper Plateau: 12,531 craters; Lower Plateau: 3642 craters; Debris Aprons: 6530 craters; Smooth Plains: 5606 craters.